Coherent Crosstalk Noise Analyses in Ring-based Optical Interconnects

Luan H.K. Duong[†], Mahdi Nikdast[‡], Jiang Xu[†], Zhehui Wang[†], Yvain Thonnart[§], Sébastien Le Beux[‖], Peng Yang[†], Xiaowen Wu[†], and Zhifei Wang[†]
[†]The Hong Kong University of Science and Technology, [‡]École Polytechnique de Montréal
[§]CEA LETI, France, [‖]Lyon Institute of Nanotechnology, France.

***Abstract*—Recently, optical interconnects have been proposed for ultra-high bandwidth and low latency inter/intra-chip communication in multiprocessor systems-on-chip (MPSoCs). These optical interconnects employ the microresonators (MRs) to direct/detect the optical signal. However, utilized MRs suffer from intrinsic crosstalk noise and power loss, degrading the network efficiency via the signal-to-noise ratio (SNR). In this paper, both coherent and incoherent crosstalk in wavelength-division multiplexing (WDM) networks are discussed and systematically analyzed. We carefully develop our analytical models at the optical-circuit level, and apply them to two ring-based networks: SUOR and Corona ONoCs. The quantitative results have demonstrated that the architectural design of the ONoCs determines the impact of crosstalk on the SNR. Even though SUOR and Corona are both ring-based ONoCs, the worst-case SNR can be differed up to 50dB. Our analyses of the worst-case SNR can be utilized as a platform to compare the realistic performance among different optical interconnection networks via the degradation of BER and data bandwidth.**

I. Introduction

With the increasingly high demand for computational performance, Networks-on-Chip (NoCs) have been introduced to replace the traditional interconnects. As more applications require higher computation power, and hence a larger number of processing cores, the metallic interconnects of NoCs could hardly meet the high-bandwidth and low-latency demands. Fortunately, this issue has been addressed by Optical Networks-on-Chip (ONoCs) with different topologies. Among those toplogies, ring-based ONoCs [1]–[4] have been proposed for ultra-high on-chip bandwidth with on-chip optical crossbars. These on-chip optical crossbars can improve the network latency because electrical-optical/optical-electrical converters are only needed at the end of the opened ring [1], [5].

Recent developments of optical interconnects have demonstrated the advantage of utilizing on-chip Wavelength-Division Multiplexing (WDM) for the interconnection in ONoCs [1], [4]. By integrating a large number of wavelengths into the network, ultra-high bandwidth data communication can be achieved. Nonetheless, crosstalk noise may be a critical issue when crosstalk is intensified among many optical components, depending on their arrangement in the ONoCs. Particularly for WDM optical interconnects, crosstalk noise from different wavelengths may affect the detected signal on a wavelength.

Fundamentally, crosstalk noise can be classified as two types: coherent and incoherent crosstalk. Indeed, [6] has given a case study on the crosstalk in ring-based WDM ONoCs. However, it solely focused on incoherent crosstalk with an analysis of the data channel and the broadcast bus in one ring-based ONoC: the Corona. In this paper, we formally provide analyses of both coherent and incoherent second-order crosstalk noise. At the optical-circuit level, we systematically model the basic optical elements to analyze the signal power loss and crosstalk noise. Having these analytical models, we utilize two different ring-based WDM ONoCs - Corona and SUOR (Sectioned Undirectional Optical Ring for Chip Multiprocessor) as our two case studies [1], [4]. With this bottom-up approach, all analytical models at the network level can be translated into initial device-level models for verification. Finally, the quantitative results of the worst-case SNR and crosstalk noise are provided, with the exploration of different dimensions such as the MR Q-factors or the passing loss. Based on the SNR results, we also present a comparison between the ideal and real bandwidth, as well as the power needed for sending a bit of data.

The rest of the paper is organized as follows: Section II briefly discusses the state-of-the-art of previous works, while Section III details our models for the basic optical elements. Section IV gives detailed analyses of the worst-case power loss and crosstalk noise in two ONoCs, followed by Section V which provides our results and discussion. Finally, Section VI draws a conclusion to this paper.

II. Summary of Related works

At the device level, crosstalk noise has often been considered negligible. For example, crosstalk noise of -47.4dB was reported by Chen, *et al.* via a waveguide crossing, which consisted of three cascaded multimode structures [7]. Another work, by Tsarev, *et al.*, also reported negligible loss and crosstalk noise [8]. Nonetheless, recently, the crosstalk noise issue has been increasingly investigated because of its negative impact on the network. [9] and [10] demonstrated this negative impact by investigating folded-torus based and mesh-based ONoCs under a single-wavelength constraint. Among the most recent works on the crosstalk noise in WDM networks, Duong, *et al.* reported the destructive effect of crosstalk on the SNR in the data channel and the broadcast bus of Corona ONoC [6]. In this works, however, only incoherent crosstalk noise was considered and analyzed. Additionally, S. Xiao, *et al.* researched a multi-wavelength micro-ring based structure and reported the losses [11].

This work is partially supported by DAG11EG05S.

III. Analysis of Crosstalk noise in Optical Elements

A. Lorentzian power transfer function

Microresonators (MRs) are intensively employed to construct optical interconnects. The MR can be coupled to two waveguides and utilized as a switching element (Fig. 1). The MR can also be coupled to a single waveguide, forming a modulator or a detector to respectively modulate or detect the optical signal (Fig. 2). Generally, the MR is approximated as a Lorentzian power transfer function which is peaked at the MR's resonant wavelength λ_{MR}. For an optical signal having wavelength λ_i, the drop-port power transfer can be expressed as (1a) [11].

In (1a), κ_e^2 and κ_d^2 are respectively the fraction of the optical power that the input and the drop waveguide coupled into or out of the MR, while κ_p^2 is the fraction of the intrinsic power losses per round-trip in the MR. To simplify our analytical equations in the later stages, we also define this ratio as $\Phi(i,j)$ as in (2). Based on recent works, for an MR, $\kappa_e^2 = 0.003$, $\kappa_d^2 = 0.001$ and $\kappa_p^2 = 0.0025$ [12]. In (1a), the -3dB bandwidth of 2δ is expressed as (1b), where Q is the Q-factor of a particular MR.

We also consider the Free-Spectral Range (FSR) of a signal via the difference between the MR's resonant wavelength λ_{MR} and the examined signal wavelength λ_i. Taking the two wavelengths λ_i and λ_j for example, we have $\Delta(i,j) = \lambda_i - \lambda_j = (i-j)(\frac{FSR}{n})$, where we assume equal spacing between two consecutive wavelengths and n is the total number of wavelengths in the network. In this paper, Q-factor is set at 9,000 [5] and FSR is assumed to be 62nm [13].

$$\frac{P_{drop}}{P_{in}} = (\frac{2\kappa_e\kappa_d}{\kappa_e^2+\kappa_d^2+\kappa_p^2})^2(\frac{\delta^2}{(\lambda_i-\lambda_{MR})^2+\delta^2}) \quad (1a)$$

$$2\delta = \frac{\lambda_j}{Q} \quad (1b)$$

$$\Phi(i,j) = (\frac{2\kappa_e\kappa_d}{\kappa_e^2+\kappa_d^2+\kappa_p^2})^2(\frac{\delta^2}{(\lambda_i-\lambda_j)^2+\delta^2}) \quad (2)$$

B. Crosstalk noise in the Optical elements

In optical interconnects, crosstalk noise is an intrinsic characteristic of photonic devices. It is classified as coherent and incoherent. Basically, we consider the crosstalk incoherent when the optical propagation delay differences in the network exceed the coherent time of the laser. Otherwise, we consider it coherent. [14] has proved that coherent crosstalk may either contribute to the noise or cause fluctuation in the signal power, depending on the propagation delay differences when being compared with the time duration of one bit of the optical signal. In this work, we consider the case that the coherent crosstalk causes noise.

To verify the impact of crosstalk noise in the optical interconnects, we utilize SNR, expressed in (3), as the ratio between the received signal and the crosstalk noise power at the detectors. In (3), SNR is indeed independent of the input signal power since the input power of the signal power and the crosstalk noise power cancel each other out. As mentioned before, the noise power in the denominator includes both coherent and incoherent crosstalk. Besides this, in order to facilitate the understanding of our analytical equations, Table I provides all the notations and data used in the analyses. The data, which are a projection towards the optical interconnect technology in 2020, are considered from recent works on Corona and Corona-like ONoCs [15]–[18].

TABLE I. Utilized Parameters Table

Parameter	Sym.	Value
Propagation loss	L_p	-0.274dB/cm
Bending loss	L_b	-0.005dB/90^o
Power loss: INACTIVE modulator	L_{m_0}	-0.005dB
Power loss: ACTIVE modulator	L_{m_1}	-0.6dB
Power loss: PASSING detector	L_{d_0}	-0.005dB
Power loss: DETECTING detector	L_{d_1}	-1.6dB
Power loss: OFF-state injector	L_{i_0}	-0.005dB
Power loss: ON-state injector	L_{i_1}	-0.5dB
Power loss: 1x2 splitter	$L_{s_{12}}$	-0.2dB
Power loss: 1x4 splitter	$L_{s_{14}}$	-0.2dB
Crosstalk coefficient: INACTIVE modulator	X_{m_0}	-16dB
Crosstalk coefficient: ACTIVE modulator	X_{m_1}	-16dB
Crosstalk coefficient: PASSING detector	X_{d_0}	-16dB
Crosstalk coefficient: DETECTING detector	X_{d_1}	-16dB
Crosstalk coefficient: OFF-state injector	X_{i_0}	-20dB
Crosstalk coefficient: ON-state injector	X_{i_1}	-25dB

$$SNR = \frac{P_{signal}}{P_{noise}} \quad (3)$$

C. Optical Injectors

Injectors are the MRs coupled into two waveguides. An injector performs as a switching element to change the light direction. Fig. 1 demonstrates its two stages: the OFF- and ON- state. In Fig. 1, the injector is injecting wavelength λ_j.

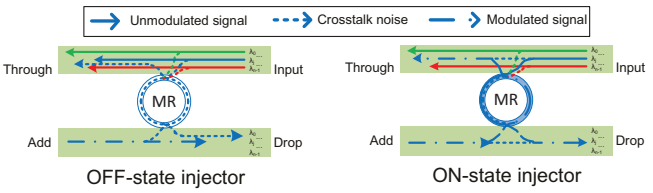

Fig. 1. Basic optical elements: Injectors/Switching elements

In the OFF-state, when the MR is off, the signal travels toward the through port. In this case, the signal power at the through port and drop port are (4a) and (4c) respectively. Due to the imperfection of the coupling mode, a portion of light from all the wavelengths can be leaked into the drop port. This crosstalk noise power is incoherent and denoted by (4d). Meanwhile, the crosstalk noise power at the through port (4b) is from the signal at the add port. This crosstalk noise is coherent if the signal from the add port and input port are generated by the same source, otherwise it is incoherent. Meanwhile, (4e) is the coherent crosstalk also at the through port. Similarly, we can derive the equations for the injector in the ON state.

In this state, the signal of wavelength λ_j is directed to the drop port. Hence, the signal power and incoherent noise at the through port are (5a) and (5c) respectively. Other optical signals are directed toward the through port, and their signal power are denoted by (5b). For the drop port, the signal power is (5d), while the noise is from two sources: the noise from other wavelengths (5e) and the noise from the optical signal at the add port (5f).

$$P_{s,T,off}[i] = L_{i_0} P_{in}[i] \qquad (i = 0, 1, ..., n-1) \tag{4a}$$

$$P_{n,T,off}[j] = (X_{i_0}^2) P_{add}[j] \tag{4b}$$

$$P_{s,D,off}[j] = L_{i_0} P_{add}[j] \qquad (i = 0, 1, ..., n-1) \tag{4c}$$

$$P_{n,D,off}[i] = \begin{cases} 0 & (i \neq j) \\ X_{i_0} P_{in}[i] + \sum_{k=0}^{n-1} \Phi(k,i) P_{in}[k] & (k \neq i) \end{cases} \tag{4d}$$

$$P_{n-coh,T,off}[i] = (X_{i_0}^2) P_{in}[i] \qquad (i = 0, 1, ..., n-1) \tag{4e}$$

$$P_{s,T,on}[i] = L_{i_0} P_{in}[i] (i \neq j) \tag{5a}$$

$$P_{s,T,on}[j] = L_{i_1} P_{in}[i] \tag{5b}$$

$$P_{n-inc,T,on}[j] = X_{i_1} P_{in}[j] \tag{5c}$$

$$P_{s,D,on}[j] = L_{i_1} P_{in}[j] \tag{5d}$$

$$P_{n,D,on,1}[j] = \sum_{i=0}^{n-1} \Phi(i,j) P_{in}[i] (i \neq j) \tag{5e}$$

$$P_{n,D,on,2}[j] = X_{i_1} P_{add}[j] \tag{5f}$$

D. Optical Modulators and Detectors

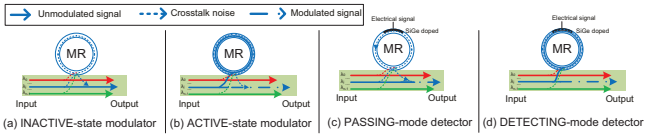

Fig. 2. Basic optical elements: Modulators and Detectors

Similar to injectors, modulators and detectors also follow the Lorentzian transfer function. They are formed by coupling the MRs to a single waveguide. Fig. 2 demonstrates different states of the modulators and detectors. Similar analyses can be applied, and equations (6) and (7) are derived for the modulators in the INACTIVE and ACTIVE states, respectively. Meanwhile, (8a) and (8b) are for photo-detectors in the PASSING mode, and (9a), (9b) and (9c) are for the detectors in the DETECTING mode. Regarding the coherent crosstalk, we take into account the portion of power which can be leaked out from the leaked-in power of the MR. (10) is derived for the coherent noise in both INACTIVE-state modulators and PASSING-mode detectors; while (11) is the for ACTIVE-state modulators and DETECTING-mode detectors.

$$P_{out}[i] = L_{m_0} P_{in}[i] \qquad (i = 0..n) \tag{6}$$

$$\begin{cases} P_{out}[j] & = X_{m_1} P_{in}[j] \\ P_{out}[i] & = L_{m_0} P_{in}[i] \quad (i \neq j) \end{cases} \tag{7}$$

$$P_{out}[i] = L_{d_0} P_{in}[i] \qquad (i = 0..n) \tag{8a}$$

$$P_{n-inc} = X_{d_0} P_{in}[j] + \sum_{i=0}^{n-1} \Phi(i,j) P_{in}[i] \qquad (i \neq j) \tag{8b}$$

$$\begin{cases} P_{out}[j] & = X_{d_1} P_{in}[j] \\ P_{out}[i] & = L_{d_0} P_{in}[i] \quad (i \neq j) \end{cases} \tag{9a}$$

$$P_{signal} = L_{d_1} P_{in}[j] \tag{9b}$$

$$P_{n-inc} = \sum_{i=0}^{n-1} \Phi(i,j) P_{in}[i] \ (i \neq j) \tag{9c}$$

$$P_{n-coh} = (X_{m_0}^2) P_{in}[j] + X_{m_0} \sum_{i=0}^{n-1} \Phi(i,j) P_{in}[i] \tag{10}$$

$$P_{n-coh} = (X_{m_1}^2) P_{in}[j] + X_{m_0} \sum_{i=0}^{n-1} \Phi(i,j) P_{in}[i] \tag{11}$$

IV. Analysis of the Worst-case Crosstalk Noise in Ring-based ONoCs

A. The worst-case Crosstalk noise in Corona ONoC

1) Overview of Corona: Corona consists of 256 general purpose cores grouped into 64 four-core clusters. Three structures are established, including: optical crossbar for data communication, broadcast bus for multi-casting, and arbitration for protocol. The main laser source is fed into the loop and split into these different structures. For each optical structure, sets of MRs perform as modulators, detectors and injectors. Table II details the optical elements of the three structures of Corona ONoC.

2) The worst-case signal power loss and crosstalk noise: In the Corona ring architecture, the control arbitration plays a critical role in avoiding congestion in the communication of the optical crossbar and the broadcast bus. In the control arbitration, the token ring methodology is utilized [1]. In this work, the data control arbitration is analyzed.

As light pulses are used for token rings, clock propagation is considered with a clock-wise movement of the data waveguide [1]. Hence, cluster 0 is the first to inject its token ring into the waveguide, followed by cluster 1, and so on until the last cluster. However, it should be noted that there exists a case where one cluster finishes its communication on almost all clusters and injects those tokens into the waveguide.

From our analyses, Fig. 3(c) demonstrates the worst-case signal power loss and SNR in the control arbitration. The optical signal suffers the highest power loss when cluster 0 injects the red token, which is detected at cluster 63's MR. This signal power is $P_{s,C0}$ in (12),where $NI0$ and $ND0$ are respectively the number of injectors and detectors which the light signal passes to reach cluster 63's detector. Meanwhile, the worst-case crosstalk noise happens when cluster 62 injects the signal of all the other 62 clusters (except cluster 0). In

this worst-case, the noise come from the following sources. The first source, expressed as (13a), is the coherent crosstalk leaked into the MRs from clusters 1 to 62. NIi and NDi are respectively the number of injectors and detectors which the signal passes when being injected from cluster i and arriving at cluster 63's detector. The other source of crosstalk noise is the incoherent noise from other wavelengths injected by cluster 62 and is detected at cluster 63 (13b). In all the equations for Corona and SUOR, L_b^* and L_p^* are used as a term for the bending and propagation losses respectively. The exact number of bendings and the distance travelled can be derived from the architectures of the two ONoCs.

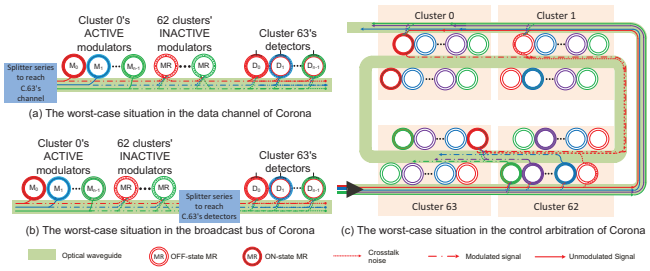

Fig. 3. Worst-case Power loss and SNR in Corona ONoC

$$P_{s,C0} = L_{i_1}(L_{i_0})^{NI0}(L_{d_0})^{ND0}L_p^*L_b^*P_{in}[0] \quad (12)$$

$$P_{n-coh} = \sum_{i=1}^{62}(L_{i_0})^{NIi}(L_{d_0})^{NDi}(L_{d_1})(L_p^*)(L_b^*)P_{in}[0] \quad (13a)$$

$$P_{n-inc} = \sum_{i=1}^{n-1}\Phi(i,0)(L_{i_1})(L_{i_0}^{63+i})(L_{d_0}^{i})L_p^*L_b^*P_{in}[i] \quad (13b)$$

Regarding the data channel and broadcast bus in Corona, they are only formed by a series of modulators and detectors. Unlike the control arbitration, splitters are also present. In our analysis, we have also considered signal power loss from these splitters. Fig. 3(a) and (b) demonstrate the worst-case communication of the data channel and broadcast bus in Corona respectively. In the data channel, the worst-case situation happens at the last cluster (i.e. cluster 63). For the broadcast bus, the worst-case situation is when the last cluster detects a multi-cast message. Also, the splitter systems are not the same: while the data channel consists of 1×2 and 1×4 splitters, the broadcast bus only consists of 1×2 splitters. The incoherent crosstalk in both structures is generated by the ACTIVE-state modulators, and the coherent is from INACTIVE-state modulators. At the end of the data and broadcast, a series of detectors is also placed to detect the modulated signal, and incoherent crosstalk is also generated.

B. The worst-case Crosstalk noise in SUOR ONoC

1) Overview of SUOR: SUOR, Sectioned Undirectional Optical Ring for Chip Multiprocessor, is another ring-based ONoC introduced in this work as the second case study. Similar to the ring structure of Corona ONoC, the SUOR network is also arranged in a network of 8×8-clusters. Each cluster consists of four cores. These 64 clusters are interconnected by a number of waveguides in order to form a closed ring. The SUOR also utilizes microresonators to perform as basic switching or detecting elements to direct or detect the light signal for data communication [4]. Table II summarizes the SUOR's optical elements in comparison with those of the Corona ONoC. From Table II, the number of waveguides and the number of MRs in SUOR are both higher than those in Corona. However, this higher number of MRs does not necessarily result in higher signal power loss in SUOR.

TABLE II. SUMMARY OF SUOR AND CORONA ONOC

Optical structure	Waveguides	Wavelengths per waveguide	MRs
SUOR: Data channel	284	64	1363548
Corona: Data channel	256	64	1048576
Corona: Broadcast bus	1	64	8192
Corona: Data control	1	64	8192

Besides the similarities, there exist differences between SUOR and Corona ONoCs. First of all, in SUOR ONoC, the broadcast bus is not included, and the control network is point-to-point (i.e. centralized). As a result, we focus our analyses on the data channel of SUOR. The 64 clusters of SUOR ONoC is slightly differently arranged compared to Corona ONoC. Furthermore, compared to Corona ONoC with only one off-chip laser source, SUOR utilizes the on-chip laser, providing power by placing VCSELs at every cluster. Besides this, SUOR has several special attributes, including: undirectional (i.e. bidirectional) transmission, channel segmentation, channel grouping and adaptive power control [4]. We have taken into consideration the first three properties in our analyses on SUOR.

2) The worst-case signal power loss and crosstalk noise in SUOR: In this part, we investigate the worst-case signal power loss and crosstalk noise of the data channel in SUOR ONoC. Different from Corona ONoC, the data channel of SUOR is divided into different channel groups with different communication length. From the analyses of the basic optical elements, it is derived that the data channel group 5 of SUOR suffers the most signal power loss. That is, the communication link between cluster i and cluster $(i+32)\ mod\ 64$, where i can be any cluster from cluster 0 to cluster 63. Fig. 4 demonstrates this link, which is a representative of group 5.

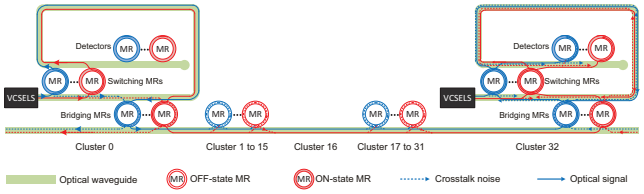

Fig. 4. The worst-case in SUOR: channel group 5

Since it is in channel group 5, only clusters with a 32-hop distance can be a sender. The other clusters can either be receivers or non-receivers (i.e. the clusters which do not have any detectors to receive the incoming light signal). In Fig. 4, when C0 sends a signal to C32, the light signal passes through 30 clusters with 64 inactive detectors each, and one cluster (i.e. cluster 16) with no MR. The signal power loss is expressed in

(14), where L_b^* and L_p^* are respectively the bending loss and the propagation loss of the link.

$$P_{signal[i]} = (L_b^*)(L_p^*)(L_{i_1})^4(L_{i_0})^{63\times 2} (L_{d_0})^{64\times 30}(L_{d_0})^i(L_{d_1})^1 P_{VCSELS}[i] \quad (14)$$

Based on our analyses of the optical elements, the worst-case crosstalk noise also happened in group 5. The crosstalk noise is generated from the four following sources. The first incoherent crosstalk is generated from the signal at the detector series at the end of the receiving cluster (i.e. cluster 32). This crosstalk can be derived from the signal power loss and the detectors of cluster 32. Incoherent crosstalk can also be generated by the signal from cluster 32 (Cluster 32 can send a signal to cluster 0 at the same time as cluster 0 sends data to cluster 32). At the bridging injectors of cluster 32, this signal generates crosstalk noise, which arrives at the series of detectors of the same cluster, 32, in the second order. This crosstalk is denoted in (15a). Regarding coherent crosstalk, it is generated by the switching MRs of cluster 0 (the sending cluster). This first order coherent crosstalk, denoted in (15b), will travel to the left of the ring and arrive at cluster 32 from the right (Fig. 4). Another coherent crosstalk is from the PASSING-mode of the detectors of other clusters and is denoted in (15c).

$$P_{n-inc[i]} = (L_b^*)(L_p^*)(L_{i_1})(L_{i_0})^{63}(X_{i_1}) (L_{i_0})^{63-i}(L_{i_1})(L_{d_0})^i(L_{d_1})^1 P_{VCSELS}[i] \quad (15a)$$

$$P_{n-coh1[i]} = (L_b^*)(L_p^*)(X_{i_1})(L_{i_1})^2 (L_{i_0})^{63\times 2}(L_{d_0})^{64\times 30}(L_{d_0})^i(L_{d_1})^1 P_{VCSELS}[i] \quad (15b)$$

$$P_{n-coh2[i]} = (L_b^*)(L_p^*)(X_{d_0}^2)(L_{i_1})^2 (L_{i_0})^{63\times 2}(L_{d_0})^{64\times 30}(L_{d_0})^i(L_{d_1})^1 P_{VCSELS}[i] \quad (15c)$$

V. Results and Comparison

Based on our analyses and the data in Table I, we provide and discuss the quantitative results of the Corona and SUOR ONoCs. By varying the important factors, such as the MR passing loss and the Q-factor, we explore different dimensions of the worst-case results. We also utilize the stated die size of 423mm^2 [1] for Corona, resulting in a chip size of 2.05cm×2.05cm. For a fair comparison, we assume the same chip size for SUOR. However, it should be noted that our analytical equations are independent of the utilized data, which are only used as an example to indicate several numerical results.

Fig. 5 demonstrates the impact of coherent crosstalk on the worst-case SNR in different structures of SUOR and Corona. As can be seen, the coherent crosstalk may significantly affect the worst-case SNR in the data channel and the broadcast bus of Corona. In these two structures, the coherent crosstalk noise dominates since it is generated by the series of INACTIVE-state modulators along the waveguide, while the incoherent crosstalk is only generated by the ACTIVE-state modulators of the first cluster. A similar trend is also applied to the control arbitration of Corona, where the coherent crosstalk far outweigh the incoherent crosstalk. On the SUOR ONoC, as the incoherent crosstalk contributes more to the noise (i.e. the

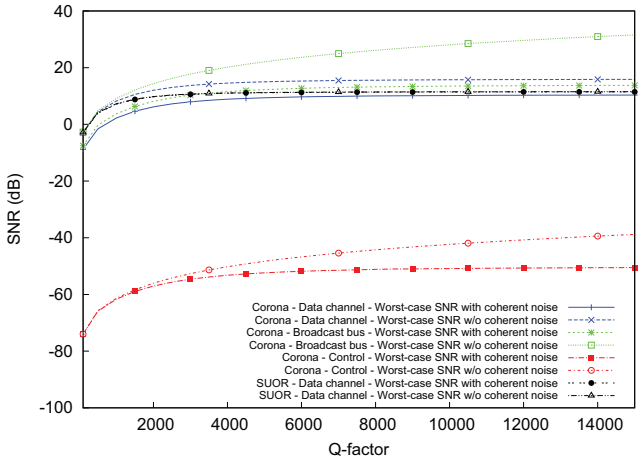

Fig. 5. The worst-case SNR, with and without coherent crosstalk when Q varies

incoherent crosstalk from cluster 32), the SNR results are not greatly reduced. Moreover, at a particular Q-factor, the worst-case SNR among the structures can differ by up to 50dB. For example, at Q=9,000, the worst-case SNR of the control arbitration in Corona is -51dB, while that of the broadcast bus in Corona is 13.38dB. Fig. 5 also demonstrates the worst-case SNR under varied Q-factors. Based on our analytical model, it can be seen that the Q-factor of an MR can significantly affect the SNR. As can be seen from Fig. 5, small Q-factors highly damage the SNR (i.e., SNR is smaller than 0 when Q is smaller than about 1000). Additionally, larger Q-factors than 15,000 may not improve the SNR since the SNR tends to gradually settle at a value when the Q-factor reaches 14,000.

In order to further investigate the impact of both incoherent and coherent crosstalk, we also vary the values of the MR passing loss (Fig. 6). Under different passing losses, the worst-case SNR of Corona is more stable, while that of SUOR ONoC decreases deeply. On the one hand, in Corona, by utilizing the off-chip laser with only one laser source, the signal as well as its crosstalk noise in a channel will pass by a similar number of MRs. Hence, under different MR passing losses, the worst-case SNR in Corona ONoC is steady. On the other hand, in SUOR ONoC, the worst-case SNR quickly decreases with an increasing MR passing loss. Particularly, the worst-case SNR is above 16dB when the passing loss is -0.001dB, but it is only above 2dB when the passing loss is -0.01dB. This trend of the SNR can be explained by the usage of a laser source in SUOR ONoC. Unlike Corona, SUOR utilizes on-chip laser sources, meaning that different clusters have different power sources on different data channels. As a result, the crosstalk noise generated from cluster 32 itself can outperform and suppress the signal reaching cluster 32 from cluster 0, resulting in a reduction of the SNR in SUOR.

We provide the results of the ideal/real bandwidth and power consumption per data bit in Table III. Regarding the ideal case, a modulation rate of 10Gbit/s is assumed [1]. The worst-case bandwidth results from the worst-case SNR of each structure. In this paper, two sets of the worst-case bandwidth have been calculated. The first set, based on the Shannon limit (16), is the maximum theoretical bandwidth which can be

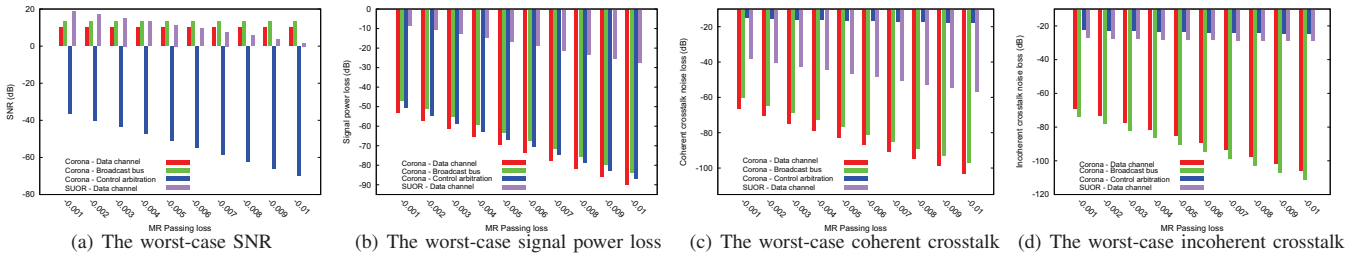

(a) The worst-case SNR (b) The worst-case signal power loss (c) The worst-case coherent crosstalk (d) The worst-case incoherent crosstalk

Fig. 6. The worst-case SNR, signal power loss and coherent and incoherent crosstalk noise under varied MR passing losses

TABLE III. IDEAL AND ACTUAL PERFORMANCE: CORONA AND SUOR

Optical structure	Ideal (no crosstalk)		Worst-case (SNR-based)			
	Bandwidth (Tb/s)	Energy (pJ/bit)	BER	Bandwidth (Tb/s)		Energy (pJ/bit)
				Shannon limit	RS(255,149)	
SUOR: Data channel	160	0.005	0.03	118.85	93.49	0.01
Corona: Data channel	160	137.50	0.04	114.19	93.49	235.32
Corona: Broadcast bus	0.64	34.19	0.02	0.5	0.37	58.51
Corona: Data control	0.64	71.42	N/A	N/A	N/A	N/A

achieved under the constraint of crosstalk noise. The second set is the bandwidth which is achieved by Reed-Solomon (RS) error correction coding. The input bit error rate (BER), expressed by (17), is achieved from the worst-case SNR [10], and RS(255,149) is chosen to reduce this BER of 10^{-2} to an output BER of 10^{-12}. In the worst-case energy consumption, the overhead of the error correction coding is not considered.

In this section, we have demonstrated that our analyses of the worst-case SNR can be a platform to compare the performance of different structures. The results have indicated that in the real situation, several structures may work, but several may not. Due to the accumulation of coherent crosstalk on the receiver, Corona's control arbitration apparently demonstrates an extremely low SNR value, hence very high BER value.

$$C = BW \times log_2(1 + \frac{Signal}{Noise}) \tag{16}$$

$$BER = \frac{1}{2} e^{-\frac{SNR}{4}} \tag{17}$$

VI. CONCLUSION

In this work, we have developed analytical models to calculate the signal power loss, crosstalk noise and SNR in a WDM network. In our analyses, both coherent and incoherent crosstalk noise are analyzed. Utilizing our developed models at the device level, we have provided the analyses of the worst-case SNR and crosstalk noise in two ring-based ONoCs: Corona and SUOR. The quantitative results demonstrate the impact of crosstalk noise on the SNR and network performance. The worst-case SNR strongly depends on the network architecture. Hence, our analyses can provide a platform to compare the realistic performance among various optical interconnects.

REFERENCES

[1] D. Vantrease, R. Schreiber *et al.*, "Corona: System implications of emerging nanophotonic technology," in *35th International Symposium on Computer Architecture*, 2008, pp. 153–164.

[2] R. W. Morris and A. K. Kodi, "Design of on-chip networks using microring-resonator based nanophotonic crossbar for future multicores," in *23rd Annual Meeting of the IEEE Photonics Society*, 2010, pp. 558–559.

[3] S. Le Beux, J. Trajkovic *et al.*, "Optical Ring Network-on-Chip (ORNoC): Architecture and design methodology," in *DATE*, 2011.

[4] X. Wu, J. Xu *et al.*, "Suor: Sectioned undirectional optical ring network for chip multiprocessors," in *ACM Journal of Emerging Technologies*, 2014.

[5] J. Ahn, M. Fiorentino *et al.*, "Devices and architectures for photonic chip-scale integration," *Applied Physics A*, vol. 95, no. 4, pp. 989–997, 2009.

[6] L. Duong, M. Nikdast *et al.*, "A case study of signal-to-noise ratio in ring-based optical networks-on-chip," *Design Test, IEEE*, vol. PP, no. 99, pp. 1–1, 2014.

[7] C. H. Chen, "Waveguide crossings by use of mutlimode tapered structures," in *21st Annual Wireless and Optical Communications Conference (WOCC), 2012*, 2012, pp. 130–131.

[8] A. V. Tsarev, "Efficient silicon wire waveguide crossing with negligible loss and crosstalk," *Opt. Express*, vol. 19, no. 15, pp. 13 732–13 737, Jul. 2011.

[9] M. Nikdast, J. Xu *et al.*, "Systematic analysis of crosstalk noise in folded-torus-based optical networks-on-chip," *IEEE Transactions on Computer-Aided Design of Integrated Circuits and Systems*, vol. 33, no. 3, pp. 437–450, Mar 2014.

[10] Y. Xie, M. Nikdast *et al.*, "Crosstalk noise and bit error rate analysis for optical network-on-chip," in *Design Automation Conference , 47th ACM/IEEE*, 2010, pp. 657–660.

[11] S. Xiao, M. H. Khan *et al.*, "Modeling and measurement of losses in silicon-on-insulator resonators and bends," *Opt. Express*, vol. 15, no. 17, pp. 10 553–10 561, 2007.

[12] V. Van, P. Absil, J. Hryniewicz, and P.-T. Ho, "Propagation loss in single-mode gaas-algaas microring resonators: measurement and model," *Journal of Lightwave Technology*, vol. 19, no. 11, pp. 1734–1739, Nov 2001.

[13] Q. Xu, B. Schmidt *et al.*, "Cascaded silicon micro-ring modulators for wdm optical interconnection," *Opt. Express*, vol. 14, no. 20, pp. 9431–9435, Oct 2006.

[14] Y. Shen, K. Lu *et al.*, "Coherent and incoherent crosstalk in wdm optical networks," *Journal of Lightwave Technology*, vol. 17, no. 5, pp. 759–764, May 1999.

[15] P. Dong, W. Qian *et al.*, "Low loss silicon waveguides for application of optical interconnects," in *IEEE Photonics Society Summer Topical Meeting Series*, 2010, pp. 191–192.

[16] F. Xia, L. Sekaric *et al.*, "Ultracompact optical buffers on a silicon chip," *Nat Photon*, vol. 1, no. 1, pp. 65–71, 2007.

[17] J. Chan, G. Hendry *et al.*, "Physical-layer modeling and system-level design of chip-scale photonic interconnection networks," *IEEE Transactions on Computer-Aided Design of Integrated Circuits and Systems*, vol. 30, no. 10, pp. 1507–1520, 2011.

[18] A. Joshi, C. Batten *et al.*, "Silicon-photonic clos networks for global on-chip communication," in *3rd ACM/IEEE International Symposium on Networks-on-Chip*, 2009, pp. 124–133.